Load Frequency Control of Time-Delayed Power System Based on Event-Triggered Communication Scheme

Xing-Chen Shangguan[a,b,c], Yong He[a,b,c], Chuan-Ke Zhang[a,b,c], Lin Jiang[d,*], Min Wu[a,b,c]

[a]*School of Automation, China University of Geosciences, Wuhan 430074, China*
[b]*Hubei Key Laboratory of Advanced Control and Intelligent Automation for Complex Systems, Wuhan, 430074, China*
[c]*Engineering Research Center of Intelligent Technology for Geo-Exploration, Ministry of Education, Wuhan 430074, China*
[d]*Department of Electrical Engineering and Electronics, University of Liverpool, Liverpool, L69 3GJ, United Kingdom*

Abstract

In frequency regulation of power grids, conveying observations to controllers and obtaining control outputs depend greatly on communication and computation resources. Particularly for modern power system with an open communication network, the costs of communication and computation should not be ignored. This paper investigates an event-triggered based load frequency control for time-delayed power system with an open communication network. Based on the lifting technique in the sampled-data control theory, a new control scheme, using both a large sampling period and a maximized threshold parameter, is introduced to further lessen communication and computation costs while preserving a desired H_∞ robust performance. The delay-dependent stability criterion of the proposed control scheme is less conservative, which takes fully the time delay, the sampling period, and the threshold parameter of event-triggered communication scheme into account. The proposed criterion is unified and can be transformed to the stability conditions of the existing research by setting different values of time delay, sampling and threshold parameter. Additionally, the usage of a large and aperiodic sampling period complies with the aperiodic updating characteristic of 2-4s in control signals in load frequency control scheme. Case studies based on a one-area power system, a two-area power system and an IEEE 39-bus benchmark test system are carried out. The simulation tests demonstrate that the proposed control scheme further reduces the communication and computation costs and ensures the load frequency control system stable operation with a preset H_∞ robust performance.

Keywords: Power system, Load frequency control, Event-triggered, Sampling period, Time delay, Communication and computation costs

1. Introduction

Load frequency control (LFC) plays an important role in frequency regulation of power system [1]. The main function of LFC is to remain the balance between load consumption and power generation in the power system, so as to maintain the frequency and the tie-line power in the system at a predetermined value [2]. LFC schemes in traditional power systems use the dedicated communication channels to detect and transmit measurement and control signals [3]. The high penetration of intermittent renewable energies, such as wind energy and solar energy, promote the increased use of demand-side response, where open communication networks are preferred than the dedicated ones. The demand-side response usually has huge number of small capacity units and operates in a market environment to increase the flexibility of whole power system [4]. Moreover, the development of a smart grid and an effective power system market highly needs an open communication infrastructure to support the increasing decentralized property of control services such as LFC, as stated in [5]. The open communication infrastructure will also allow a bilateral contract for the provision of load following and third party LFC [6]. As reported in [7], the open communication network has been widely used in LFC of modern power systems.

Modern power systems are evolving towards a new generation of smart grid, where the increasing deployment of phase measurements units (PMUs) and smart meters leads to a substantial increase of measurements/control signals in the open communication network [8]. With the large-scale deployment of these information technology infrastructures, the tremendous data exchange would rapidly make the network load imbalanced and exhaust the network resources [9]. The power network operators have to face the communication bottlenecks, leading to unreliable operations of power system [10]. Moreover, as reported in

☆This work was supported in part by the National Natural Science Foundation of China under Grants 62022074, 61973284 and 61873347, by the Hubei Provincial Natural Science Foundation of China under Grants 2019CFA040, and by the 111 project under Grant B17040.

*Corresponding author
Email address: ljiang@liverpool.ac.uk (Lin Jiang)

[11], the communication between generation units also has bandwidth constraints in practical LFC. Therefore, it is desirable to design an effective LFC scheme that can stay the balance between load and generation while consuming less communication and computation resources.

An event-triggered (ET) communication scheme performs well in reducing the communication network burden in the smart grids, as stated in [12] and [14]. For instance, In the economic dispatch, an ET communication-based distributed optimization was proposed to reduce information exchange requirements [10]. Liu et al. [15] developed an ET particle filter to relieve the communication burden in the distributed generation system, while Yang et al. introduced a dynamic event-triggered robust secondary frequency control for islanded AC microgrid to provide a good balance between dynamic performance and communication burden [13]. On the other hand, under the same bandwidth, using less bandwidth will help the communication system provide more communication channels to transmit measurement/control signals for the control system at the same time, which can improve the redundancy and reliability of the LFC system. This facilitates the application of the ET communication schemes into the LFC systems, and much attention has been paid to the event-trigged-based LFC (ETLFC) scheme [17].

On the other hand, time delays are unavoidable during signal processing and transmission, and can degrade the control performance of the system and may threaten the stability of the system [18]. As to the open communication networks, such delays are uncertain due to factors such as communication protocol, network loading, and routing over different types of communication lines [20]. For example, Peng et al. [21] suggested that time delays vary within [0.15, 2] seconds in LFC systems when an open communication network is used, while Andersen et al. found about 3 seconds during the field tests when a multi-layer communication network is used for frequency control [22]. Additionally, the packet losses caused by the cyber-attacks or communication failures can be converted to an equivalent time-varying delay [3]. If some cyber-attacks or the communication failures exist, the time delays will be larger. As pointed out in [23], time delay dependent stability analysis of the LFC is still useful for the extreme case of cyber-attacks or even the communication faults from the communication networks even if the dedicated communication channels are employed. Therefore, the time-delay stability analysis of LFC scheme has been paid much attention.

Peng et al. [21] investigated LFC of power systems with probabilistic interval time delays, while a new method was put forward for the closed-loop stability analysis of PI-type LFC scheme with interval time-varying delay [24]. Additionally, from the perspective of reducing computational complexity of the time-delay stability condition, Jin et al. proposed the structure-exploiting technique-based and the model reconstruction technique-based stability analysis conditions for the large-scale LFC system [19]. The stability conditions for LFC system of these references are all based on the continuous control environment. However, the practical LFC system is a sampled-data control system, where the control signal update period is usually 2-4s, as stated in [25] and [20]. These references all ignore the practical sampling characteristics of load frequency control system. As pointed out in [34], the existence of sampling period will affect the accuracy of time-delay stability analysis. Therefore, considering the sampling characteristic, the load frequency control schemes with fast frequency response dynamic performance and robust performance are designed respectively in Refs. [36] and [37]. In addition, Ref. [20] further explored the time-delay stability of load frequency control system. In consideration of sampling characteristics and to reduce communication burden, the method of increasing sampling period was proposed in [36] and [37]. Moreover, to further save communication and computation resources, the ET communication scheme is widely used in LFC systems, as mentioned in the above. When using the ETLFC schemes, the triggered signals are selected by the ET condition, and may not withstand the same upper bound of the time delay that the signals can withstand in the LFC without the ET scheme. It can be predictable that the control performance of the LFC system will be degraded if the effective and important signals triggered by ET condition are subject to these delays. Therefore, it is desirable to explore the delay-dependent ETLFC.

Recently, the delay-dependent ETLFC system have been widely studied. In 2016, Wen et al. [16] firstly presented the H_∞ ETLFC scheme for power systems with the communication delay to reduce the transmission amount of measurement/control signals while preserving the desired H_∞ robustness performance. Whereafter, many scholars have done a lot of work to improve the ETLFC scheme. Their research endeavors can be summarized as three aspects. The one is to reduce the conservatism of the delay-dependent stability condition of the ETLFC system. In [26], the Wirtinger-type integral inequality was used to estimate the derivative of the Lyapunov functional instead of the usage of the free-weight-matrix technique in [16]. As an improvement, an exponential and discrete Lyapunov functional considering the sampling characteristics was constructed in [27] compared with the continuous Lyapunov functionals chosen by [16] and [26]. The second is to improve the control performance of the ETLFC scheme. Several effective control methods have been introduced into LFC scheme, including the slide mode control [28], the multi-agent-based optimal control [29], the model-based control [30], the model predictive control [31], the L_2 robust control [17] and the adaptive dynamic programming [8]. The last is to further reduce the communication burden. The adaptive ETLFC schemes have been developed in [26] and [27], where the threshold parameter can be adaptively adjusted to save more limited network resources. Additionally, a switched-based ETLFC scheme was presented in [17], where the amount of sent mea-

surement is reduced by switching between periodic sampling and continuous ET. In addition to the above research, some resilient ETLFC schemes under cyber-attacks were proposed to lighten the burden of network bandwidth while preserving a required H_∞ robust performance in [32].

However, there are some gaps in the above research. First of all, most scholars do not deeply explore the stability of the system considering time delay, sampling period and threshold parameters. Only few scholars in [16], [26] and [27] proposed some theorems to determine the stability of an ETLFC system considering the sum of sampling period and time delay. Second, these stability theorems are relatively conservative, which will affect the effectiveness of controller design and reducing communication and computation costs. The conservatism is due to two aspects. The one is that the way of taking the sum of time delay and sampling period ignores the sawtooth-like characteristic of the sampling period [33]. Fridman et al. [34] pointed out that the delay-dependent stability of a sampled-data system can be significantly affected by sampling period. Another one is that the choose of the Lyapunov functional. Zeng et al. [35] stated that a two-side looped functional can effectively reduce the conservatism of the stability condition for a sampled-data system in comparison with the usage of the one-side looped functional in the above research. Lastly, as stated in [25], a practical LFC is a sampled-data system, where the power commands sent to generation units are updated 2–4 s. In the existing research, the sampling period is regarded as a small value (less than one second), and it does not match the normal value in the practical LFC system. Therefore, it is necessary to explore the delay-dependent stability of ETLFC system considering a large and aperiodic sampling period. In response to the large sampling of control signals, the sampling period of measurements should also be increased. It can be expected that the communication burden can be further reduced through both the usage of large sampling period and the maximized threshold parameter in the ET scheme. These gaps motivate our research.

Based on the above discussions, this paper investigates the delay-dependent stability of the ETLFC scheme of power system. The ETLFC model of power system equipped with PI-type controller is built firstly. Then, an improved delay-dependent stability condition is proposed for the ETLFC scheme based on a lifting technique and a two-side looped Lyapunov functional. Next, the methods of reducing communication and computation costs are introduced. Finally, the effectiveness of the proposed methods is verified by case studies based on a one-area power system, a two-area power system and an IEEE 39-bus benchmark test system. In summary, the main contributions are as follows.

1) Different from the methods based on only the ET scheme in [26, 27, 32] or only the large sampling period in [36, 37], a new method, using both a large sampling period and a maximal threshold parameter, is presented to save more communication and computation resources under a given PI controller and a preset H_∞ robust performance index.
2) A new delay-dependent stability criterion for ETLFC is proposed, and it is less conservative in comparison with the existing conditions in [16, 26, 27]. The criterion, which considers uncertain time delay, aperiodic sampling period and threshold parameter separately, is taken in a continuous-time model but derived by a discrete-time two-side looped Lyapunov functional.
3) The proposed stability criterion is unified and can be converted into the stability conditions of the delay-dependent LFC scheme in [38, 2, 39], the sampled-data-based LFC scheme in [36] and the sampled-data-based delay-dependent LFC scheme in [20, 37].
4) To comply with the aperiodic characteristic of 2–4s in control signal updating of the LFC scheme, the proposed stability condition ensures the stable operation of the ETLFC system under a large and aperiodic sampling period.

The remainder of this paper is organized as follows. Section 2 presents the ETLFC model of power system. Section 3 proposes the delay-dependent stability analysis method for the ETLFC scheme. In Section 4, a method of saving communication and computation costs is introduced. Section 5 is the case studies to validate the effectiveness of the proposed scheme. Conclusions are presented in Section 6.

2. Modeling ETLFC scheme for power system

In this section, a dynamic model of ETLFC of power system is introduced. This model considers the sampling characteristic and time delay in an open communication network.

2.1. The LFC model of power system

A multi-area power system comprises N subareas that are interconnected by tie-lines. For every subarea i, the similar linearized model is presented in Fig. 1, which includes the governor, the turbine, the rotating mass and load, the tie-line power and the communication channel, where ΔP_{ci}, ΔP_{vi}, ΔP_{mi}, ΔP_{di}, Δf_i and ΔP_{tie-i} denote the deviation of the controller output, the valve position, the generator mechanical output, the load, the frequency and the tie-line power exchange of the i_{th} area of the power system, respectively; β_i, R_i, M_i, D_i, T_{chi} and T_{gi} are the frequency bias factor, the speed drop, moments of inertia of the generator, damping coefficient of the generator, time constant of the turbine and time constant of the governor of the i_{th} area of the power system, respectively; T_{ij} is the tie-line synchronizing coefficient between area i and area j, and $v_i = \sum_{j=1,j\neq i}^{N} T_{ij}\Delta f_j$; ACE_i represents the area control error (ACE) of the i_{th} area and is the linear combination of Δf_i and ΔP_{tie-i}, i.e., $ACE_i = \beta_i \Delta f_i + \Delta P_{tie-i}$.

For the multi-area power system, the decentralized control strategy is applied. The interactions between different

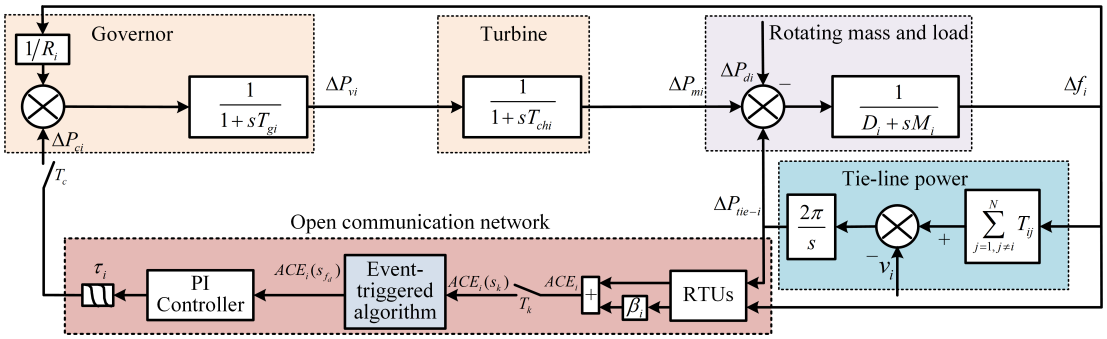

Figure 1: ETLFC structure of i_{th} area of a multi-area power system.

areas, v_i, are treated as disturbances for every area. This means that every control area is independent and has its own LFC center to maintain the balance of generation and load. Assume that the generator in every subarea is equipped with non-reheat turbine. Then, recall the LFC model in [36] and define $\tilde{x}_i = [\Delta f_i, \Delta P_{tie-i}, \Delta P_{mi}, \Delta P_{vi}]^T$, $\tilde{y}_i = ACE_i$, and $\tilde{\omega}_i = [\Delta P_{di}, v_i]^T$. One can obtain the following LFC model of i_{th} area of the power system

$$\begin{cases} \dot{\tilde{x}}_i(t) = \tilde{A}_i\tilde{x}_i(t) + \tilde{B}_i\tilde{u}_i(t) + \tilde{F}_i\omega_i(t) \\ \tilde{y}_i(t) = \tilde{C}_i\tilde{x}_i(t) \end{cases} \tag{1}$$

where

$$\tilde{A}_i = \begin{bmatrix} -\frac{D_i}{M_i} & -\frac{1}{M_i} & \frac{1}{M_i} & 0 \\ 2\pi\sum_{j=1,j\neq i}^{N} T_{ij} & 0 & 0 & 0 \\ 0 & 0 & -\frac{1}{T_{chi}} & \frac{1}{T_{chi}} \\ -\frac{1}{R_i T_{gi}} & 0 & 0 & -\frac{1}{T_{gi}} \end{bmatrix}$$

$$\tilde{B}_i = \begin{bmatrix} 0 & 0 & 0 & \frac{1}{T_{gi}} \end{bmatrix}^T, \ \tilde{C}_i = [\,\beta_i \ \ 1 \ \ 0 \ \ 0\,]$$

$$\tilde{F}_i = \begin{bmatrix} -\frac{1}{M_i} & 0 & 0 & 0 \\ 0 & -2\pi & 0 & 0 \end{bmatrix}^T.$$

Choose the following PI-type controller

$$\tilde{u}_i(t) = -K_{Pi}ACE_i(t) - K_{Ii}\int ACE_i(t) \tag{2}$$

where K_{Pi} and K_{Ii} are the proportional gains and integral gains, respectively.

In the ET LFC scheme, the common supervisory control and data acquisition system (SCADA) is employed to receive and dispatch the measurement/control signals, where the remote terminal units (RTUs) are used for acquisition of the measurements (Δf_i and ΔP_{tie-i}). The transmission instants s_k ($k = 1, 2, 3, \cdots$) of RTUs are synchronized among the sensors in different areas of power systems. These measurements are sent out at a time interval T_k. The sequence of $\{s_k\}$ is strictly increasing and goes to infinity as k goes. There exist two positive scalars $h_1 < h_2$ such that the difference between two successive sampling instants $T_k = s_{k+1} - s_k$ satisfies

$$\forall k \geq 0, 0 < h_1 \leq T_k \leq h_2. \tag{3}$$

Then, through the ACE filtering and signal processing in the control center, the control signal of the power commands are sent to generation units by a time interval T_c usually within $[2, 4]s$. To simplify the modeling, assume that: T_k is equal to T_c. The delays, including network-induced delays and fault-induced delays, are combined as one single delay $\tau_i(t)$, which is uncertain and time-varying with lower bound τ_m and upper bound τ_M and satisfies

$$0 \leq \tau_m \leq \tau_i(t) \leq \tau_M, |\dot{\tau}_i(t)| \leq \mu < 1. \tag{4}$$

where μ is the upper bound of the derivative of time delay. Especially, if $\dot{\tau}_i(t) = 0$, then $\tau_i(t)$ is constant and $\tau_m = \tau_M$. Additionally, assume that the multiple delays $\tau_i(t)$ with $i = 1, 2, ..., N$ are all equal and considered as a single delay $\tau(t)$.

As shown in Fig. 1, $ACE_i(t)$ cannot be directly used due to the sampling of measurements, the ET scheme, and the time delay in the open communication network. Then, the attainable $ACE_i(t)$ at the LFC center can be written as follows:

$$ACE_i(t) = ACE_i(s_k), t \in [s_k + \tau(s_k), s_{k+1} + \tau(s_{k+1})) \tag{5}$$

Denoting $t_k = s_k + \tau(s_k)$ as the updating instants of the control input $u_i(t)$, for $t \in [t_k, t_{k+1})$, the PI controller can be rewritten as

$$\tilde{u}_i(t) = \tilde{u}_i(s_k) = -K_{Pi}ACE_i(s_k) - K_{Ii}\int ACE_i(s_k). \tag{6}$$

Define $x_i(t) = [\tilde{x}_i^T(t) \int \tilde{y}_i^T(t)]^T$ and $y_i(t) = [\tilde{y}_i^T(t) \int \tilde{y}_i^T(t)]^T$. Then the closed-loop LFC model of the i_{th} area can be rewritten as

$$\begin{cases} \dot{x}_i(t) = A_i x_i(t) - B_i K_i C_i x_i(t_k - \tau(s_k)) + F_i\omega(t) \\ y_i(t) = C_i x_i(t), \qquad t \in [t_k, t_{k+1}) \end{cases} \tag{7}$$

where

$$A_i = \begin{bmatrix} \tilde{A}_i & 0 \\ \tilde{C}_i & 0 \end{bmatrix}, B_i = \begin{bmatrix} \tilde{B}_i \\ 0 \end{bmatrix}, C_i = \begin{bmatrix} \tilde{C}_i & 0 \\ 0 & 1 \end{bmatrix}, F_i = \begin{bmatrix} \tilde{F}_i \\ 0 \end{bmatrix},$$

$K_i = [K_{Pi} \ K_{Ii}]$.

2.2. The delay-dependent ETLFC model

Firstly, the ET communication scheme is revisited [26]. The ET condition is defined as

$$\partial_1(j) = y_{ei}^T(s_{f_d+j})\varpi_i y_{ei}(s_{f_d+j}) - \delta_i y_i^T(s_{f_d})\varpi_i y_i(s_{f_d}) \leq 0 \tag{8}$$

where $y_{ei}(s_{f_d+j}) = y_i(s_{f_d+j}) - y_i(s_{f_d})$ (j=1,2,...); $f_d (d = 0, 1, 2, \ldots)$ are some integers; s_{f_d} represents the last event time; δ_i is a threshold parameter; and ϖ_i is a positive define weighting matrix. The next event-time instant $s_{f_{(d+1)}}$ is determined by

$$s_{f_{(d+1)}} = s_{f_d} + \min_{j\in\mathbb{N}}\{s_{f_d+j} - s_{f_d} | \partial_1(j) > 0\} \tag{9}$$

Combining with $y_i(t) = C_i x_i(t)$, (8) can be rewritten as

$$\partial_2(j)=x_{ei}^T(s_{f_d+j})\Omega_i x_{ei}(s_{f_d+j})-\delta_i x_i^T(s_{f_d})\Omega_i x_i(s_{f_d})\leq 0 \quad (10)$$

where $x_{ei}(s_{f_d+j}) = x_i(s_{f_d+j}) - x_i(s_{f_d})$ and $\Omega_i = C_i^T \varpi_i C_i$. Note that the threshold parameter δ needs to be positive. The event-triggered condition $\partial_2(j) > 0$ is always valid when $\delta = 0$. Under this case, the signal trigger mechanism is the same as the time-triggered mode.

Based on the ET scheme, the PI control law can be written as

$$u_i(t)=u_i(s_{f_d})=-K_i y_i(s_{f_d})=-K_i C_i x_i(s_{f_d}),\ t\in\Pi \quad (11)$$

where $\Pi = [t_{f_d}, t_{f_{(d+1)}})$ with $t_{f_d} = s_{f_d} + \tau(s_{f_d})$. Similar to [26], the interval Π is divided into the following subsets Π_l,

$$\Pi=\bigcup\Pi_l,\ \ \Pi_l=[t_{f_d+l}, t_{f_d+(l+1)}) \quad (12)$$

where $l = 0, 1, \ldots, f_{(d+1)} - f_d - 1$, and

$$\tau(s_{f_d+l})=\begin{cases}\tau(s_{f_d}), l=0,1,\ldots,f_{(d+1)}-f_d-2\\ \tau(s_{f_{(d+1)}}), l=f_{(d+1)}-f_d-1\end{cases} \quad (13)$$

Define $\varsigma(t) = t - (t_{f_d+l} - \tau(s_{f_d+l}))$, $t \in \Pi_l$. The control law (11) can be rewritten as

$$u_i(t)=K_i C_i(x_{ei}(s_{f_d+l})-x_i(t-\varsigma(t))),\ t\in\Pi_l \quad (14)$$

Then, by replacing (6) with (14), the state space model of delay-dependent ETLFC for a multi-area power system can be formulated as

$$\begin{cases}\dot{x}_i(t)=A_i x_i(t)+B_i K_i C_i(x_{ei}(s_{f_d+l})-x_i(t-\varsigma(t)))+F_i\omega_i(t)\\ y_i(t)=C_i x_i(t),\ t\in\Pi_l\end{cases} \quad (15)$$

The length of interval Π_l, $\bar{T}_{f_d+l} = t_{f_d+(l+1)} - t_{f_d+l}$, satisfies

$$\forall l\geq 0, 0<\bar{h}_1\leq\bar{T}_{f_d+l}\leq\bar{h}_2<2h_2 \quad (16)$$

where $\bar{h}_1 = h_1 - \min(\tau_M - \tau_m, \mu h_1)$ and $\bar{h}_2 = h_2 + \min(\tau_M - \tau_m, \mu h_2)$. Note that $|\dot{\tau}(t)| \leq \mu < 1$ ensure that $|\tau(s_{f_d+(l+1)}) - \tau(s_{f_d+l})| < \bar{T}_{f_d+l}$ and then the sequence of t_{f_d+l}'s is strictly increasing. Especially, when the delay is constant, i.e., $\tau_m = \tau_M$ and $\mu = 0$, $\bar{T}_{f_d+l} \in [h_1, h_2]$, $\bar{h}_1 = h_1$ and $\bar{h}_2 = h_2$. Moreover, if the delay is constant and the sampling is periodic, i.e., $h_1 = h_2$, then $\bar{T}_{f_d+l} = h_1 = h_2 = \bar{h}_1 = \bar{h}_2$.

3. Stability Criterion of Delay-Dependent ETLFC for power system

In this section, a novel stability criterion is proposed for delay-dependent ETLFC scheme of power system. Threshold parameter, uncertain time delay and aperiodic sampling period are all considered to analyze the stability of ETLFC of power system.

3.1. The delay-dependent stability criterion of ETLFC

Theorem 1: Consider system (15) with zero disturbance. For given $T_k \in [h_1, h_2]$, $\tau_i \in [\tau_m, \tau_M]$ with $|\dot{\tau}_i(t)| \leq \mu < 1$, δ_i and K_i, system (15) is asymptotically stable if there are positive definite symmetric matrices P, M, N, H, R_1, R_2 and Ω_i, and any appropriately dimensioned matrices Q_1, Q_2, X, Z, U_1 and U_2 such that, for $j = 1, 2$, the following inequalities hold:

$$\Xi_1=\begin{bmatrix}\Theta_1+\bar{h}_j\Theta_2 & \bar{h}_j U_2\\ * & -\bar{h}_j R_2\end{bmatrix}<0 \quad (17)$$

$$\Xi_2=\begin{bmatrix}\Theta_1+\bar{h}_j\Theta_3 & \bar{h}_j U_1\\ * & -\bar{h}_j R_1\end{bmatrix}<0 \quad (18)$$

where

$$\begin{aligned}\Theta_1=&e_1^T M e_1 - e_2^T M e_2 + E_0^T N E_0 - e_3^T N e_3 + \tau_M E_0^T H E_0\\ &-\frac{1}{\tau_M}\Pi_3^T\begin{bmatrix}H & 0\\ 0 & 3H\end{bmatrix}\Pi_3+Sym\{\Pi_1^T P\Pi_{21}+\Pi_{71}^T Q_1\Pi_{72}\\ &+\Pi_{71}^T Q_2\Pi_8+\Pi_2^T X(\Pi_4-\Pi_6)+(\Pi_4-\Pi_5)^T X\Pi_2\\ &-U_1(\Pi_4-\Pi_5)+U_2(\Pi_4-\Pi_6)\}\\ &+\delta_i(e_5-e_9)^T\Omega_i(e_5-e_9)-e_9^T\Omega_i e_9\\ \Theta_2=&Sym\left\{\begin{bmatrix}\Pi_2\\ 0\end{bmatrix}^T Q_1\Pi_{72}+\begin{bmatrix}\Pi_4-\Pi_5\\ 0\end{bmatrix}^T Q_1\begin{bmatrix}\Pi_2\\ \Pi_2\end{bmatrix}\right\}\\ &+Sym\left\{\begin{bmatrix}\Pi_2\\ 0\end{bmatrix}^T Q_2\Pi_8\right\}+\Pi_8^T Z\Pi_8+\Pi_2^T R_1\Pi_2\\ \Theta_3=&Sym\left\{\begin{bmatrix}0\\ \Pi_2\end{bmatrix}^T Q_1\Pi_{72}+\begin{bmatrix}0\\ \Pi_4-\Pi_6\end{bmatrix}^T Q_1\begin{bmatrix}\Pi_2\\ \Pi_2\end{bmatrix}\right\}\\ &+Sym\left\{\begin{bmatrix}0\\ \Pi_2\end{bmatrix}^T Q_2\Pi_8\right\}-\Pi_8^T Z\Pi_8+\Pi_2^T R_2\Pi_2\\ E_0=&Ae_1+BKC(e_9-e_5),\ \Pi_1=[e_1^T\ e_2^T\ \tau_M e_8^T]^T\\ \Pi_2=&[E_0^T\ e_3^T]^T,\ \Pi_{21}=[\Pi_2^T\ (e_1-e_2)^T]^T\\ \Pi_3=&[(e_1-e_2)^T\ (e_1+e_2-2e_8)^T]^T\\ \Pi_4=&[e_1^T\ e_2^T]^T,\ \Pi_5=[e_4^T\ e_5^T]^T,\ \Pi_6=[e_6^T\ e_7^T]^T\\ \Pi_{71}=&[(\Pi_5-\Pi_4)^T\ (\Pi_4-\Pi_6)^T]^T\\ \Pi_{72}=&[(\Pi_4-\Pi_5)^T\ (\Pi_4-\Pi_6)^T]^T,\ \Pi_8=[\Pi_5^T\ \Pi_6^T]^T\\ e_i=&[0_{r\times(i-1)r}\ \ I_r\ \ 0_{r\times(9-i)r}],\ i=1,2,\cdots 9.\end{aligned}$$

with $\bar{h}_1$ and $\bar{h}_2$ defined in (16), r the dimension of matrix A in system (15) and denoting$Sym\{\mathbb{A}\} = \mathbb{A} + \mathbb{A}^T$. The proof can be found in Appendix.

Remark 1: The following techniques are involved to reduce the conservatism in comparison with the existing research in Refs. [16, 26, 27]: 1) In the construct of Lyapunov functional, the terms of time delays are constructed into $V_1(\cdot)$, and the terms of the sampling period are constructed into $V_2(\cdot)$, which consider the time delay and sampling period, separately. 2) With respect to $V_2(\cdot)$, a new two-side looped-functional is introduced, where the functional fully utilizes the information on both the intervals from $z(\alpha)$ to $z(0)$ and from $z(\alpha)$ to $z(\bar{T}_\rho)$.

Remark 2: The stability condition presented is applicable to aperiodic sampling period, which is consistent with the variable updating of control signals in LFC scheme.

Remark 3: The essential difference of the stability analysis for LFC with and without ET scheme lies in the way that the measured signals are triggered. The signals are triggered based on an event in the ET scheme, while the signals are triggered based on the sampling time

T_k in LFC without ET scheme. Threshold parameters δ_i , weight matrix Ω_i and the relationship of inequality (10) need to be taken into account in stability analysis for ETLFC.

Remark 4: Theorem 1 considers the influence of time delay, sampling period and threshold parameter on the stability of the ETLFC scheme. By setting special values for the three parameters, Theorem 1 can be developed into the stability conditions of the existing research on LFC scheme, including sampled-data-based delay-dependent (SDDD) LFC scheme in [37, 20], the sampled-data-based (SD) LFC scheme in [36], and the delay-dependent (DD) LFC scheme in [38, 18, 2]. The obtained corollaries are shown as follows.

Corollary 1-1 (SDDD [20, 37]) : Theorem 1 with $\delta = 0$.

Corollary 1-2 (SD [36]): Theorem 1 with $\delta = 0$ and $\tau_m = \tau_M = 10^{-4}s$.

Corollary 1-3 (DD [2, 18, 38]): Theorem 1 with $\delta = 0$ and $h_1 = h_2 = 10^{-4}s$.

3.2. A time delay margin analysis method

To calculate the time delay margin, the inequality constraints of Theorem 1 can be transformed into the below constrained optimization problem $\mathcal{P}1$. Since problem $\mathcal{P}1$ is non-convex, the margin cannot be calculated directly via linear optimization solver. It can be developed by using the binary search technique combined with solver YALMIP in MATLAB. The detailed search procedure of the delay margin can be find in [3]. Moreover, by setting the minimum value h_1 of the sampling period and fixing the other parameters, we can obtain the margin of the sampling period by applying the similar method introduced above.

$\mathcal{P}1$:	max	τ_M
	s.t.	$P > 0$, $M > 0$, $N > 0$, $H > 0$, $R_i > 0$, $\Omega > 0$,
		$\Xi_i < 0$, $i = 1, 2$ and $j = 1, 2$.
	where	given τ_m, μ, h_1, h_2 and δ and K.

4. Design of the H_∞ ETLFC scheme to reduce communication and computation costs

In this section, a new method is proposed to save the communication and computation costs in the LFC under a fixed PI controller while preserving a desired H_∞ robustness performance.

To design the ETLFC with H_∞ robust performance, we need to ensure that system (15) with $\omega_i(t) = 0$ is asymptotically stable and under the zero initial state condition, for any nonzero $\omega_i(t) \in \mathcal{L}_2[0, \infty]$ and a preset $\gamma > 0$, the inequality $\|y_{zi}(t)\|_2 \leq \gamma\|\omega_i(t)\|_2$ holds. Assume that $y_{zi}(t) = C_{zi}x_i(t) = [\eta_i\Delta f_i(t), \varepsilon_i\int ACE_i(t)]$, and η_i and ε_i with $i = 1, \ldots, N$ are constant weighting coefficients. The fictitious outputs $\eta_i\Delta f_i(t)$ and $\varepsilon_i \int ACE_i(t)$ are introduced to minimize the impacts of input disturbances on frequency and ACE (and tie-line power flow) signals. Based on Theorem 1, one can obtain the following theorem:

Theorem 2: Considering system (15) with nonzero disturbance, for given $T_k \in [h_1, h_2]$, $\tau_i \in [\tau_m, \tau_M]$ with $|\dot{\tau}_i| \leq \mu < 1$, δ_i, K_i, η_i, and ε_i, system (15) is asymptotically stable with an H_∞ robustness index γ if there are positive definite symmetric matrices P, M, N, H, R_1, R_2 and Ω_i, and any appropriately dimensioned matrices Q_1, Q_2, X, Z, U_1 and U_2 such that, for $j = 1, 2$, satisfy the following conditions hold:

$$\hat{\Xi}_1 = \begin{bmatrix} \hat{\Theta}_1 + \bar{h}_j\Theta_2 & \bar{h}_j U_2 \\ * & -\bar{h}_j R_2 \end{bmatrix} < 0 \tag{19}$$

$$\hat{\Xi}_2 = \begin{bmatrix} \hat{\Theta}_1 + \bar{h}_j\Theta_3 & \bar{h}_j U_1 \\ * & -\bar{h}_j R_1 \end{bmatrix} < 0 \tag{20}$$

where $\hat{\Theta}_1 = \Theta_1 + e_1^T C_z^T C_z e_1 - \gamma^2 e_{10}^T e_{10}$, $e_i = [0_{r\times(i-1)r} \;\; I_r \;\; 0_{r\times(9-i)r} \;\; 0_{r\times N}]$, $i = 1, 2, \cdots 9$, $e_{10} = [0_{N\times 9r} \;\; I_N]$, and E_0 in Θ_1 is substituted with $Ae_1 + BKC(e_9 - e_5) + Fe_{10}$. The proof can be found in Appendix.

To complete the design of the proposed method, a large periodic sampling period is first selected to comply with the large and aperiodic updating characteristic of the control signals in LFC. Then, under this sampling period, the threshold parameter is maximized based on Theorem 2 under a given controller K_i and a desired H_∞ robustness index γ. Finally, both the large sampling period and the large threshold parameter are adopted to reduce the unnecessary transmission of measurement/control signals. Calculating the maximal threshold parameter can be transformed into the following constrained optimization problem $\mathcal{P}2$. The maximum of threshold parameter can be calculated by the binary search technique and the linear optimization solver YALMIP, like $\mathcal{P}1$.

$\mathcal{P}2$:	max	δ_i
	s.t.	$P > 0$, $M > 0$, $N > 0$, $H > 0$, $R_i > 0$, $\Omega_i > 0$,
		$\Xi_i < 0$, $i = 1, 2$ and $j = 1, 2$.
	where	given τ_m, τ_M, μ, h_1, h_2, γ, η_i, ε_i and K_i.

Based on the above description, the detailed design procedure of the proposed scheme can be summarised as the following Algorithm 1.

Algorithm 1: Design H_∞ ETLFC scheme with large sampling and maximum threshold parameter

Step 1: Divide the power system into N control areas. Preset system parameters A_i, B_i, C_i and F_i with $i = 1, 2, ..., N$.

Step 2: Determine the parameters of time delay τ_i and set the appropriate controller gains K_i.

Step 3: Set the desired H_∞ performance index γ, constant weighting coefficients η_i and ε_i, and sampling period T_k.

Step 4: Find the maximal threshold parameter δ_i based on Theorem 2 and $\mathcal{P}2$.

Step 5: If no feasible solution δ_i, adjust the controller gains K_i and H_∞ performance index γ. Then repeat Step 4. If exist the feasible solution, output K_i, γ and δ_i.

5. Case Studies

In this section, case studies are undertaken based on a one-area LFC system, a two-area LFC system and an

IEEE 39-bus benchmark test system to show the effectiveness and advantages of the proposed approach. In the two-area LFC system and the IEEE 39-bus test system, the PI controller gains in each area are assumed to be equal. To show the advantages of the proposed approach on reducing communication and computation costs, the following control schemes are compared in the simulation tests.

1) The time-triggered (TT) control scheme with a large sampling period in [36];
2) The event-triggered (ET) control scheme with a small sampling period and a small threshold parameter in [16];
3) The adaptive event-triggered (AET) control scheme with a small sampling period and a small threshold parameter in [26];
4) The proposed control scheme with a large sampling period and a maximal threshold parameter in this paper.

The amount of control signal update in LFC system is considered as a indicator to evaluate the consumption of communication and computing resources. In addition, we compare the conservatism of the stability analysis conditions of the proposed scheme with the existing stability analysis conditions in [16] and [26]. Their delay margins are calculated and used as an indicator to evaluate their conservatism [20].

5.1. A one-area power system

The one-area LFC system is studied and its parameters are shown in 'Area 1' of Table 1.

Table 1: Parameters of the one-area and the two-area LFC system

	T_{ch}(s)	T_g(s)	R(Hz/pu)	D(pu/Hz)	M(pu·s)	γ(pu/Hz)	T_{ij}(pu/rad)
Area 1	0.30	0.10	0.05	1.0	10	21.0	$T_{12} = 0.1986$
Area 2	0.40	0.17	0.05	1.5	12	21.5	$T_{21} = 0.1986$

5.1.1. Conservatism comparison to other stability conditions of LFC system under fixed sampling

The margins of constant time delay obtained in this paper are compared with the results developed in [16] and [26] under a periodic sampling period. Under $T_k = h_1 = h_2 = 2s$, their results are shown in Table 2 (the fixed K_I and δ and the different K_P) and Table 3 (the fixed K_P and the different K_I and δ). The symbol $'-'$ denotes cases where asymptotic stability cannot be guaranteed.

Tables 2 and 3 clearly show that the method proposed in this paper always provides a larger delay margin compared to the results obtained in [26]. Nevertheless, the results obtained in [16] are sometimes larger than the results in this paper. To verify the obtained results, time-domain simulations of the studied system are undertaken. Under a step disturbance $\Delta P_d = 0.1$ pu at $t = 0s$, the frequency deviation of the one-area LFC system with $K_P = 0.2$, $K_I = 0.6$, $\delta = 0$, $T_k = 2s$ and with $K_P = 0.05$, $K_I = \delta = 0.1$, $T_k = 2s$ under different constant time delays are shown in Figs. 2 and 3, respectively. Simulation results indicate that the delay margins in the two cases lie in the intervals [0.95, 1.27]s and [8.85, 13.8]s, respectively. This proves that the LFC system can maintain the stability at the obtained delay margins of 0.95s and 8.85s, respectively. On the other hand, it can be found that the delay margins of $1.75s$ and $22.12s$ obtained in [16] exceed the intervals [0.95, 1.27]s and [8.85, 13.8]s, and the frequency deviation in Figs. 2 and 3 are both divergent. This shows that the method proposed in [16] is incorrect. The corresponding mathematical proof is provided in the appendix.

In addition, under different parameter selection of the threshold parameter, the time delay and the sampling period, we compare the margins of time delay or sampling period obtained in Corollaries 1-1, 1-2 and 1-3 with the results developed in the existing research of SDDD [20, 37], SD [36] and DD [2], respectively. Their results are listed in Table 4. It is not difficult to find that the results obtained in this paper are not far from those obtained by the existing research. This shows that the proposed method is effective and unified.

Table 2: Margins of constant time delay of one-area LFC obtained in this paper, [26] and [16] under $\delta = K_I = 0.1$ and different K_P

K_P	0	0.05	0.1	0.15	0.2	0.3
Th1.	8.42	**8.85**	9.03	8.75	8.05	5.39
[26]	7.83	5.53	2.56	1.06	0.23	-
[16]	39.51	**21.12**	8.11	4.24	2.78	1.61

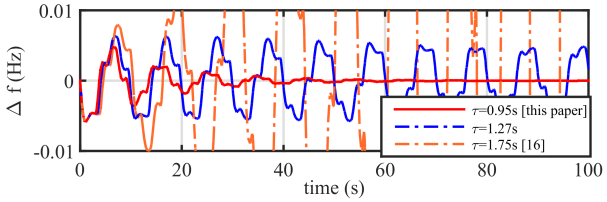

Figure 2: Frequency deviation of the one-area LFC under $T_k = 2s$, $\delta = 0$, $K_P = 0.2$, and $K_I = 0.6$ and different constant time delays.

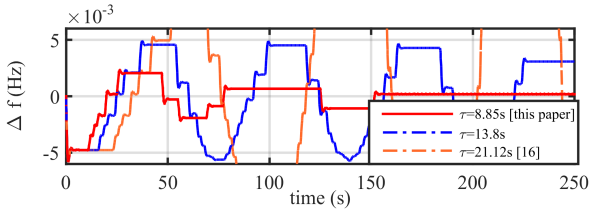

Figure 3: Frequency deviation of the one-area LFC under $T_k = 2s$, $\delta = K_I = 0.1$ and $K_P = 0.05$, and different constant time delays.

Table 4: Comparisons with the stability criteria of the one-area LFC system in [20, 36, 37, 2], under $\delta = 0$ and $K_P = 0.2$

	Margins of τ_M			Margins of h_2		Margins of τ_M	
K_I	Cor.1-1	[20]	[37]	Cor.1-2	[36]	Cor.1-3	[2]
0.05	31.43	31.87	28.17	30.61	30.85	33.90	32.76
0.1	14.71	15.30	13.52	15.57	15.63	16.61	16.80
0.2	6.49	6.77	5.89	8.10	8.20	8.08	8.14
0.4	2.36	2.45	1.97	4.59	4.57	3.76	3.78

5.1.2. Design of H_∞ ETLFC scheme

Following the steps of Algorithm 1, the time delay and the PI controller gains are set to $\tau = 2$s and $K_P = K_I =$

Table 3: Margins of constant time delay of one-area LFC obtained in this paper, [26] and [16] under $K_P = 0.2$ and different δ and K_I

	$\delta = 0$			$\delta = 0.01$			$\delta = 0.05$			$\delta = 0.1$			$\delta = 0.3$		
	Th1.	[26]	[16]	Th1.	[26]	[16]	Th1.	[26]	[16]	Th1.	[26]	[16]	Th1.	[26]	[16]
$K_I = 0.05$	31.43	1.61	4.67	27.43	1.19	3.96	22.22	0.68	3.30	18.57	-	2.94	10.42	-	2.28
$K_I = 0.1$	14.71	1.51	4.41	13.01	1.10	3.74	10.71	0.60	3.13	9.03	-	2.78	4.96	-	2.17
$K_I = 0.2$	6.49	1.20	3.79	5.64	0.83	3.22	4.51	0.36	2.72	3.67	-	2.43	1.65	-	1.91
$K_I = 0.4$	2.36	0.41	2.58	1.89	0.10	2.24	1.31	-	1.91	0.91	-	1.70	0.12	-	1.33
$K_I = 0.6$	**0.95**	-	**1.75**	0.68	-	1.50	0.41	-	1.26	0.21	-	1.11	-	-	0.81

0.1, respectively. The preset H_∞ performance index is $\gamma = 100$, respectively. Then, setting the sampling period $T_k = 4s$ and $\eta = 1, \varepsilon = 0$, the maximal threshold parameter $\delta = 0.235$ can be found based on Theorem 2 and $\mathcal{P}2$.

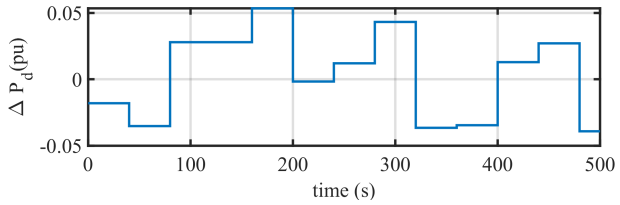

Figure 4: Random changes of load of the one-area LFC system.

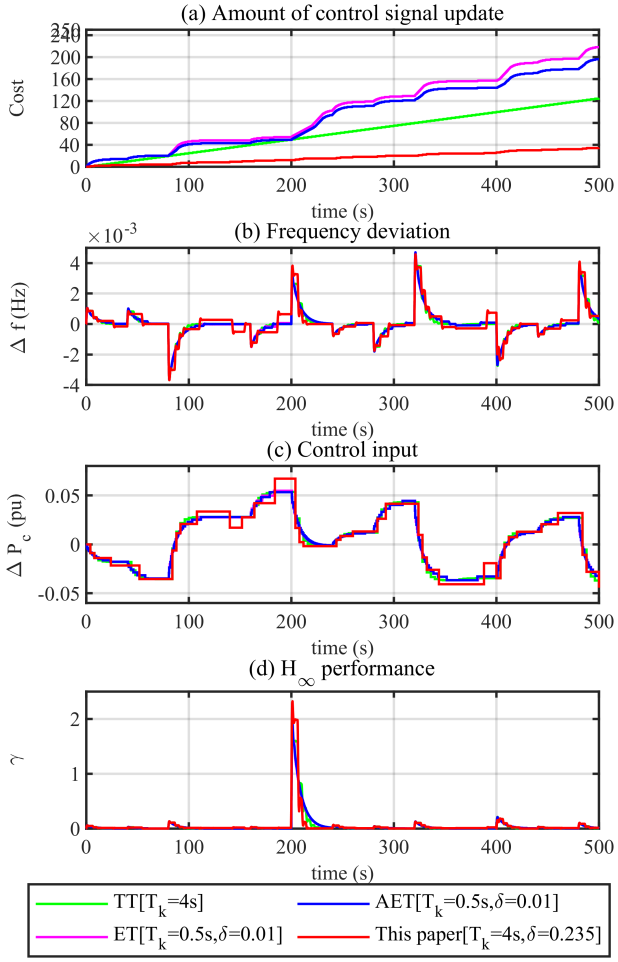

Figure 5: Communication and computation costs, frequency deviation and control input of one-area power system.

5.1.3. *Performance results and comparison with the other methods*

The studied system is tested under the TT [36], ET [16], AET [26] control schemes and the proposed control schemes when subjected to random changes of load. The random changes of load are shown in the Fig. 4.

Within 500s, the communication and computation costs, the frequency deviation, the control input and the H_∞ performance are drawn in Figs. 5 (a), (b), (c) and (d), respectively. It can be seen from Figs. 5 (a) and (c) that the proposed control scheme effectively reduces the amount of control signal update compared with other methods. This will greatly reduce the communication and computation consumption. Moving on to Fig. 5 (b), we can see that the response of the frequency deviation of the proposed control scheme is basically the same as that of other methods. Also, from Fig. 5 (d), the H_∞ performance of the proposed control scheme is almost the same as that of other methods and complies with the desired H_∞ performance requirement. These results indicate that the proposed method can further reduce the communication and computation costs while meeting the desired H_∞ performance and sacrificing a little dynamic performance in frequency response.

5.2. *A Two-area LFC system*

In this section, the two-area LFC system is evaluated, and its parameters are listed in Table 1. The generation rate constraints for every generator are considered to be ± 0.1 pu/min.

5.2.1. *Conservatism comparison to other stability conditions of LFC system under aperiodic sampling*

Assume that $\tau_m = 10^{-4}s$, $\mu = 0.5$, and $T_k \in [2, 4]$s. The upper bounds of time-varying delay are developed based on Theorem 1 under various PI controller gains and threshold parameters, and are compared with the results obtained by [26]. This comparison is summarized in Table 5 (the fixed K_I and δ and the different K_P) and Table 6 (the fixed K_P and the different K_I and δ). The results of area 1 is similar and omitted here due to space limitation.

Table 5: Upper bounds of time-varying delay of area 2 obtained in this paper and [26] under $\delta = 0.1$, and $K_I = 0.05$ and different K_P

K_P	0	0.05	0.1	0.15	0.2	0.3
Th1.	14.89	**15.23**	13.89	12.15	7.55	0.45
[26]	14.55	5.93	1.23	-	-	-

From Tables 5 and 6, it can be seen that the results obtained in this paper significantly improve the results of

[26]. Then, time-domain simulations for the two-area LFC system with uncertain time delays and aperiodic sampling period are undertaken to verify the effectiveness of the obtained results. For the sake of simulation and analysis, the transmission interval of measurements is always assumed as the worst value of 4s. Under a step disturbance $\Delta P_{d1} = 0.1$ pu and $\Delta P_{d2} = 0.06$ pu at $t = 10s$, the frequency responses of area 2 with case 1 ($K_P = K_I = 0.05$, $\delta = 0.1$, $T_k = 4s$, $\tau_1 \in [15, 15.37]s$ and $\tau_2 \in [15, 15.23]s$) and with case 2 ($K_P = 0$, $K_I = 0.2$, $\delta = 0.1$, $T_k = 4s$, $\tau_1 \in [0.9, 0.93]s$ and $\tau_2 \in [0.8, 0.88]s$) are shown in Figs. 6 (a) and (b), respectively. The upper bounds of the two cases in area 1 calculated by this paper are 15.37s and 0.93s, respectively. From Fig. 6, it can be observed that the studied system can maintain stability under the obtained upper bound of time delay, which demonstrates the effectiveness of the proposed method.

Table 6: Upper bounds of time-varying delay of area 2 obtained in this paper and [26] under $K_P = 0.1$ and different δ and K_I

	$\delta = 0$		$\delta = 0.01$		$\delta = 0.1$		$\delta = 0.3$	
	Th1.	[26]	Th1.	[26]	Th1.	[26]	Th1.	[26]
$K_I = 0.05$	27.37	4.00	23.76	3.12	13.89	1.24	4.79	-
$K_I = 0.1$	11.00	3.09	8.90	2.30	4.38	0.60	1.20	-
$K_I = 0.2$	2.15	1.03	1.82	0.44	**0.88**	-	-	-
$K_I = 0.4$	0.32	-	0.18	-	-	-	-	-

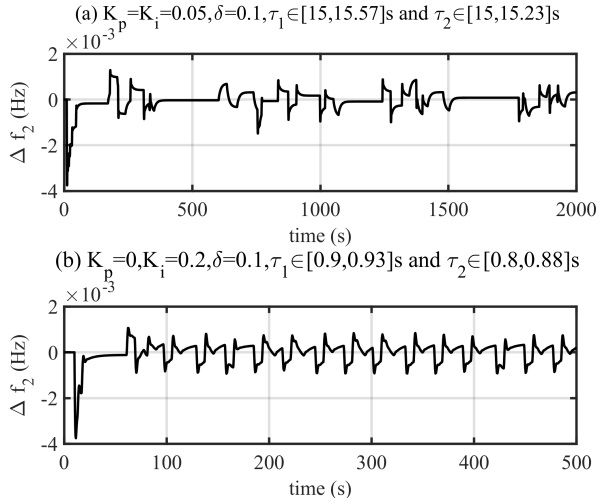

Figure 6: Frequency deviations of area 2 under cases 1 and 2.

5.2.2. Design of H_∞ ETLFC scheme

Following the steps of Algorithm 1, the time delay and the PI controller gains are assumed as $\tau_1 = \tau_2 \in [0.15, 2]$s and $K_P = K_I = 0.1$, respectively. The preset H_∞ performance index is $\gamma = 100$, respectively. Then, setting the sampling period $T_k \in [2, 4]s$ and $\eta = 1, \varepsilon = 0$, the maximal threshold parameters $\delta_1 = 0.116$ and $\delta_2 = 0.139$ in the two areas can be found based on Theorem 2 and $\mathcal{P}2$.

5.2.3. Performance results and comparison to the other methods

To show the advantages of the proposed method, the studied system is tested under the TT [36], ET [16], AET [26] control schemes and the proposed control schemes when subjected to random changes of load shown in Fig. 7 within 500s. The communication and computation costs of the two areas, the frequency deviation of area 2, the control input of area 2 and the H_∞ performance of area 2 are drawn in Figs. 8 (a), (b), (c), and (d) respectively.

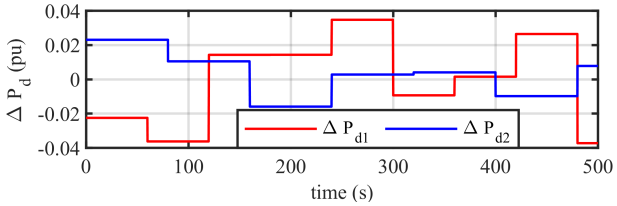

Figure 7: Random changes of load in two areas.

From Figs. 8 (a) and (c), it can be seen that the ability of the proposed scheme to reduce the communication and computation costs is superior to other methods. In addition, moving on to Fig. 8 (b), despite the significant reduction in the costs, there is only a little change of the dynamic performance in the frequency response compared with other control schemes. Also, from Fig. 8 (d), the H_∞ performance is below the required value. Therefore, these results validate that the proposed control scheme is effective.

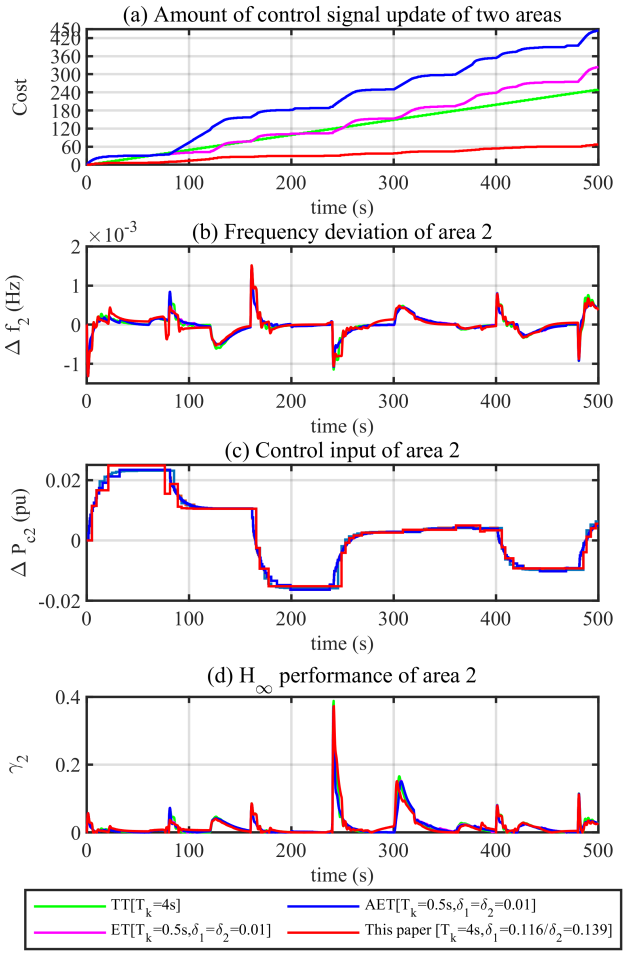

Figure 8: Communication and computation costs, frequency deviation and control input of the two-area LFC system.

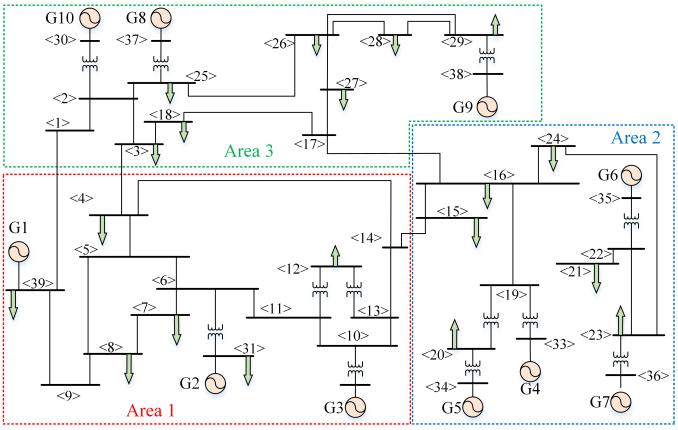

Figure 9: Single-line diagram of IEEE 39-bus test system.

5.3. An IEEE 39-bus benchmark test system

To further demonstrate the effectiveness and applicability of the proposed control system, we test it in a more complex IEEE 39-bus benchmark test system. The single-line diagram of the studied system is shown in Fig. 9. This system consists of 10 generators, 19 loads, 34 transmission lines, and 12 transformers. The generators are equipped with excitation and power system stabilizer units. The power system is divided into three control areas. Assume that every generator in each area is responsible for the secondary frequency regulation task. The simulation parameters for the generators, loads, lines and transformers are given in [41]. The generation rate constraints for every generator are considered to be ± 0.1 pu/min.

5.3.1. Conservatism comparison to other stability conditions of LFC system under fixed sampling

We compare the margins of constant time delay obtained in this paper with the results developed in [26] under fixed sampling period. The results of area 2 are listed in Tables 7 and 8. The results of area 1 and area 3 are similar and omitted here.

Table 7: Upper bounds of constant time delay of area 2 in the IEEE 39-bus test system obtained in this paper and [26] under $\delta = 0.01$, and $K_I = 0.05$ and different K_P

K_P	0	0.05	0.1	0.15	0.2	0.3
Th1.	24.74	25.68	**25.32**	14.24	4.71	0.10
[26]	9.11	0.82	-	-	-	-

Table 8: Upper bounds of constant time delay of area 2 in the IEEE 39-bus test system obtained in this paper and [26] under $K_P = 0$ and different δ and K_I

	$\delta = 0$		$\delta = 0.01$		$\delta = 0.1$		$\delta = 0.3$	
	Th1.	[26]	Th1.	[26]	Th1.	[26]	Th1.	[26]
$K_I = 0.05$	27.29	12.04	24.74	9.11	20.50	5.59	17.57	2.90
$K_I = 0.1$	13.12	3.75	11.09	2.90	8.76	1.08	7.21	-
$K_I = 0.2$	4.79	-	3.63	-	**2.46**	-	1.60	-
$K_I = 0.4$	0.77	-	0.55	-	0.19	-	-	-

From Tables 7 and 8, it is not difficult to see that the results obtained in this paper is far lager than the results of [26]. Then, time-domain simulations for the test system with case 1 ($K_P = 0.15, K_I = 0.05$, $\delta_1 = \delta_2 = \delta_3 = 0.1$, $T_k = 4s$, $\tau_1 = 12.09s$, $\tau_2 = 14.24s$ and $\tau_3 = 24.52s$) and case 2 ($K_P = 0$, $K_I = 0.2$, $\delta = 0.1$, $T_k = 4s$, $\tau_1 = 1.05s$, $\tau_2 = 2.46s$ and $\tau_3 = 2.42s$) are undertaken to verify the effectiveness of the obtained results. Under a step disturbance of $\Delta P_{d1} = 0.08$ pu, $\Delta P_{d2} = 0.06$ pu and $\Delta P_{d3} = 0.1$pu at $t = 10s$, the frequency responses of area 2 with case 1 and case 2 are depicted in Fig. 10. Note that the delay margins in area 1 and area 3 for two cases are $\tau_1 = 12.09s, \tau_3 = 24.52s$ (case 1) and $\tau_1 = 1.05s, \tau_3 = 2.42s$ (case 2). It can be seen in Fig. 10 that the frequency response curves of two cases are both converged, which indicates that the obtained results are accurate.

5.3.2. Design of H_∞ ETLFC scheme

Following the steps of Algorithm 1, the time delay and the PI controller gains are assumed as $\tau_1 = \tau_2 = \tau_3 = 2$s and $K_P = K_I = 0.05$, respectively. The preset H_∞ performance index is $\gamma = 100$, respectively. Then, setting the sampling period $T_k = 4s$ and $\eta = 1, \varepsilon = 0$, the maximal threshold parameters $\delta_1 = 0.075$, $\delta_2 = 0.038$ and $\delta_3 = 0.108$ in three areas can be calculated based on Theorem 2 and $\mathcal{P}2$.

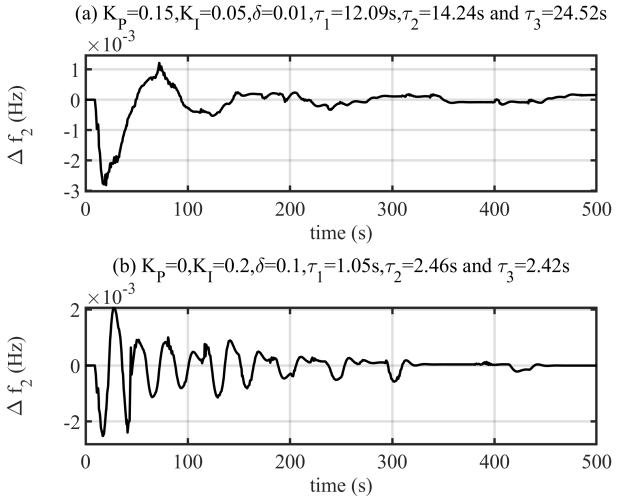

Figure 10: Frequency deviations of area 2 in the IEEE 39-bus test system under cases 1 and 2.

5.3.3. Performance results and comparison to the other methods

The system is tested under TT [36], ET [16], AET [26] control schemes and the proposed control schemes when subjected to random load disturbances within 500s. The random changes in cumulative load of every area are shown in Fig. 11. The communication and computation costs of the three areas, the frequency deviation of area 1, the control input of area 1 and the H_∞ performance of area 1 are depicted in Figs. 12 (a), (b), (c) and (d), respectively.

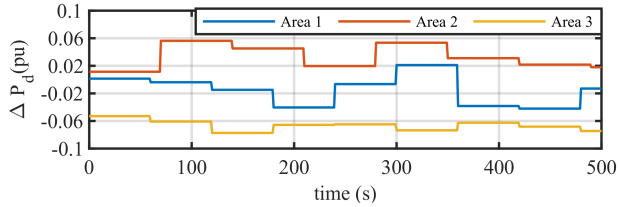

Figure 11: Random changes in cumulative load of three areas in the IEEE 39-bus test system.

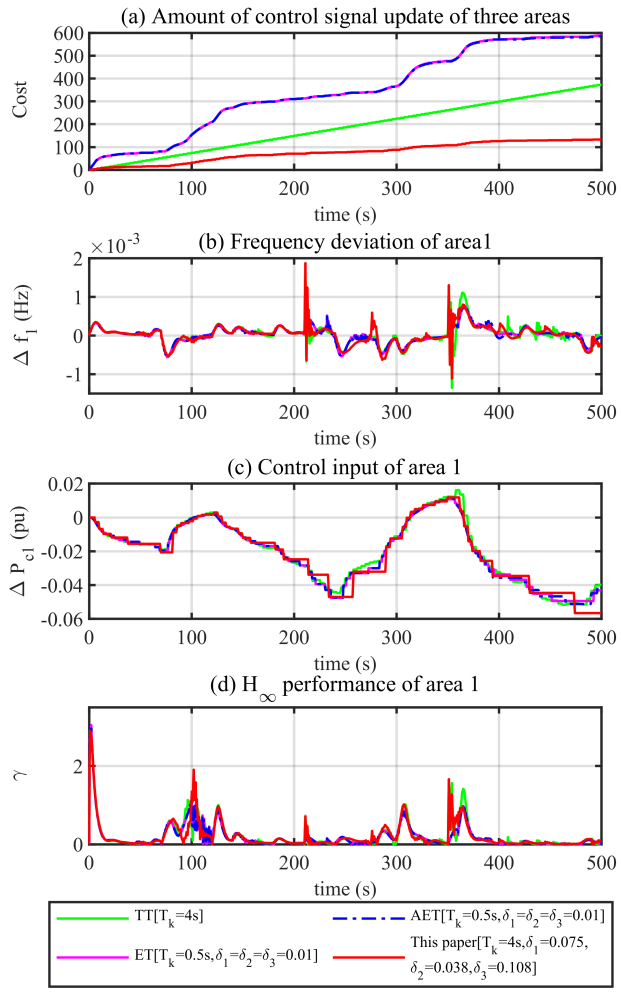

Figure 12: Random changes in cumulative load of every area in the IEEE 39-bus test system.

From these figures, we can get the same conclusions as the one-area LFC an the two-area LFC systems. The LFC system under the proposed control scheme needs to provide 120 times of control input signal update to regulate the frequency within 500s, while more than 380 times will be provided under other control schemes. This greatly reduces the amount of transmission of measurement and control signals in the communication system, the calculation resources and the adjustment action of the generator unit's equipment. Furthermore, this reduction improvement does not significantly degrade the frequency response dynamic performance, as shown in the Fig. 12 (b). In addition, the studied system can be guaranteed to run stably under the specified H_∞ performance index. The above results prove the effectiveness and superiority of the proposed scheme.

Remark 5: It can be seen from the Tables 3, 6, and 8 that with the increase of threshold parameter δ, the upper bounds of time delay that the LFC system can withstand decrease. In Table 6, this phenomenon is obvious. The upper bound of time delay is 27.37s for the LFC without ET scheme and the threshold parameter $\delta = 0$, while the upper bound is only 4.79s for the ETLFC and the threshold parameter $\delta = 0.3$. Therefore, the signals triggered by the event-triggered condition can not withstand the same upper bound of the time delay that the signals can withstand in the LFC without ET scheme. The necessity to explore the time-delay stability issue for ETLFC is illustrated by these results.

Remark 6: To achieve unified stability conditions, more system characteristics, including time delay, sampling and threshold parameter, are considered. This makes the derivation of the stability condition of the system complicated, and may cause the stability condition to be more conservative or difficult to improve the stability condition. Although the unified stability conditions are obtained in Refs. [16, 26], they are more conservative. In this paper, the lifting technique and the two-side looped Lyapunov functional are used to greatly reduces the conservatism. Similarly, on the basis of the research results in this paper, the proposed stability condition can also be improved by selecting suitable Lyapunov functional and estimating the derivative of Lyapunov functional with less conservative inequalities. For instance, the improved two-side looped Lyapunov functional constructed in [42] and the improved general free-matrix-based integral inequality proposed in [43]. This is the future research direction of the paper.

6. Conclusion

This paper has explored the load frequency control for time-delayed power system to save the communication and computation costs. The control scheme of using both the large sampling period and maximal threshold parameter has been presented to address this concern under a given proportional-integral controller and a preset H_∞ performance index. The obtained numerical results have revealed that the stability criterion of the proposed control scheme is less conservative than other stability evaluation conditions. The criterion can be transformed into the existing stability conditions by setting special values of time delay, sampling period and threshold parameter. In addition, the simulation results based on the one-area and two-area power systems and the IEEE 39-bus benchmark test system have indicated that the proposed control scheme consumed the least communication and computation costs to ensure the stable operation of the power system than other control schemes, while guaranteeing the preset H_∞ robustness performance.

Appendix

Proof of Theorem 1

To simplify the notation, $\rho = f_d + l$ is introduced. The discrete-time model of system (15) with zero disturbance is obtained by integrating the differential equation (15) over the interval $[t_\rho, t_\rho + \alpha]$, for any α in $[0, \bar{T}_\rho]$ with $\bar{T}_\rho \in [\bar{h}_1, \bar{h}_2]$,

$$\begin{array}{l} x_i\left(t_\rho+\alpha\right)=\tilde{A}_i(\alpha)x_i\left(t_\rho\right)+\tilde{A}_{id}(\alpha)(x_{ei}(s_\rho)-x_i(t-\varsigma(t))) \\ \tilde{A}_i(\alpha)=e^{A_i\alpha}, \quad \tilde{A}_{id}(\alpha)=\int_0^\alpha e^{A_i(\alpha-\theta)}d\theta B_iK_iC_i \end{array} \tag{21}$$

Then, for all integer ρ, define the function $\chi_\rho : [0, \bar{T}_\rho] \times [-\tau(s_\rho), 0] \longrightarrow \mathbb{R}^n$ such that for all α in $[0, \bar{T}_\rho]$ and all ϵ in $[-\tau(s_\rho), 0]$, $\chi_\rho(\alpha, \epsilon) = x_i(t_\rho + \alpha + \epsilon)$. Then, choose a Lyapunov-Krasovskii functional as follows

$$V(\chi_\rho) = V_1(\chi_\rho) + V_2(\alpha, \chi_\rho) \tag{22}$$

where

$$\begin{aligned} V_1(\chi_\rho) =& {\xi_1}^T P\xi_1 + \int_{-\tau(s_\rho)}^0 \chi_\rho^T(\alpha,s)M\chi_\rho(\alpha,s)ds \\ &+ \int_{-\tau(s_\rho)}^0 \dot{\chi}_\rho^T(\alpha,s)N\dot{\chi}_\rho(\alpha,s)ds \\ &+ \int_{-\tau(s_\rho)}^0 \int_\lambda^0 \dot{\chi}_\rho^T(\alpha,s)H\dot{\chi}_\rho(\alpha,s)dsd\lambda \end{aligned}$$

$$\begin{aligned} V_2(\alpha,\chi_\rho) =& Sym\left(\xi_2^T\left(Q_1\xi_3+Q_2\xi_4\right)\right)+\left(\bar{T}_\rho-\alpha\right)\alpha\xi_4^TZ\xi_4 \\ &+ Sym\left(\left(z^T(\alpha)-z^T(0)\right)X\left(z(\alpha)-z\left(\bar{T}_\rho\right)\right)\right) \\ &+ \left(\bar{T}_\rho-\alpha\right)\int_0^\alpha \dot{z}^T(s)R_1\dot{z}(s)ds \\ &- \alpha\int_\alpha^{\bar{T}_\rho} \dot{z}^T(s)R_2\dot{z}(s)ds \end{aligned}$$

with

$$z(\alpha)=[\chi_\rho^T(\alpha,0)\chi_\rho^T(\alpha,-\tau(s_\rho))]^T, \xi_1=[z^T(\alpha)\int_{-\tau(s_\rho)}^0 \chi_\rho^T(\alpha,s)ds]^T$$

$$\xi_2=[\left(\bar{T}_\rho-\alpha\right)\left(z^T(\alpha)-z^T(0)\right)\ \alpha\left(z^T(\alpha)-z^T\left(\bar{T}_\rho\right)\right)]^T$$

$$\xi_3=[z^T(\alpha)-z^T(0)\ z^T(\alpha)-z^T\left(\bar{T}_\rho\right)]^T, \xi_4=[z^T(0)\ z^T\left(\bar{T}_\rho\right)]^T$$

$$\varphi=[z^T(\alpha)\ \dot{\chi}_\rho^T(\alpha,-\tau(s_\rho))\ z^T(0)\ z^T(\bar{T}_\rho)\ \frac{1}{\tau_M}\int_{-\tau(s_\rho)}^0 \chi_\rho^T(\alpha,s)ds\ x_e^T(s_{f_d+j})]^T.$$

Note that $V_2(\alpha, \chi_\rho)$ is a looped functional, and satisfies $V_2(0, \chi_\rho) = V_2(\bar{T}_\rho, \chi_\rho) = 0$. Based on theorem 1 in [33], to guarantee the stability of system (15), the objective is here to ensure that the variation of $V_1(\chi_\rho)$ between two successive sampling instant is strictly negative. Therefore, the remainder of the proof ensures that $\dot{V}(\chi_\rho) = \frac{d}{d\alpha}\left[V_1\left(\chi_\rho(\alpha,\cdot)\right) + V_2\left(\alpha, \chi_\rho(\cdot,\cdot)\right)\right] < 0$. One can obtain:

$$\begin{aligned} \dot{V}(\chi_\rho) \leq& \varphi^T(e_1^TMe_1-e_2^TMe_2+E_0^TNE_0-e_3^TNe_3+\tau_ME_0^THE_0 \\ &+Sym\{\Pi_1^TP\Pi_{21}+\Pi_{71}^TQ_1\Pi_{72}+\Pi_{71}^TQ_2\Pi_8 \\ &+\Pi_2^TX(\Pi_4-\Pi_6)+(\Pi_4-\Pi_5)^TX\Pi_2\})\varphi \\ &+(\bar{T}_\rho-\alpha)\varphi^T\Theta_2\varphi+\alpha\varphi^T\Theta_3\varphi-\int_{-\tau(s_\rho)}^0 \dot{\chi}_\rho^T(\alpha,s)H\dot{\chi}_\rho(\alpha,s)ds \\ &-\int_0^\alpha \dot{z}^T(s)R_1\dot{z}(s)ds-\int_\alpha^{\bar{T}_\rho} \dot{z}^T(s)R_2\dot{z}(s)ds \end{aligned}$$

The first integral term of $\dot{V}(\chi_\rho)$ can be bounded by applying the Wirtinger-based integral inequality [40]:

$$-\int_{-\tau(s_\rho)}^0 \dot{\chi}_\rho^T(\alpha,s)H\dot{\chi}_\rho(\alpha,s)ds \leq -\varphi^T\left(\frac{1}{\tau_M}\Pi_3^T\begin{bmatrix}H & 0\\ 0 & 3H\end{bmatrix}\Pi_3\right)\varphi \tag{23}$$

Then, any matrices U_1 and U_2 satisfy the following zero-equations based on the free-weight-matrix technique

$$0 = 2\varphi^TU_1\left(z(\alpha)-z(0)-\int_0^\alpha \dot{z}(s)ds\right) \tag{24}$$

$$0 = 2\varphi^TU_2\left(z(\bar{T}_\rho)-z(\alpha)-\int_\alpha^{\bar{T}_\rho} \dot{z}(s)ds\right). \tag{25}$$

Next, add zero-equations (24) and (25) and the ET condition (10) into the derivative. This yields

$$\dot{V}(\chi_\rho) \leq \frac{1}{\bar{T}_\rho}\int_\alpha^{\bar{T}_\rho}\begin{bmatrix}\varphi\\ \dot{z}(s)\end{bmatrix}^T\Xi_1\begin{bmatrix}\varphi\\ \dot{z}(s)\end{bmatrix}ds+\frac{1}{\bar{T}_\rho}\int_0^\alpha\begin{bmatrix}\varphi\\ \dot{z}(s)\end{bmatrix}^T\Xi_2\begin{bmatrix}\varphi\\ \dot{z}(s)\end{bmatrix}ds \tag{26}$$

Considering the inner matrix at the right side of (26) is linear and therefore convex, with respect to $\bar{T}_\rho \in [\bar{h}_1, \bar{h}_2]$, the right side of (26) is negative definite if $\Xi_1 < 0$ and $\Xi_2 < 0$. This completes the proof.

Proof of theorem 2

Define $\hat{\varphi} = [\varphi^T w_\rho^T(\alpha, 0)]^T$, where $w_\rho(\alpha, 0) = \omega_i(t_\rho+\alpha)$. Following the proof of theorem 1, one can obtain from (19) and (20)

$$\dot{V}(\chi_\rho) \leq -C_{zi}^T\chi_\rho^T(\alpha,0)\chi_\rho(\alpha,0)C_{zi} + \gamma^2w_\rho^T(\alpha,0)w_\rho(\alpha,0)$$

Then, from $\alpha \in [0, \bar{T}_\rho]$ to $t \in [t_\rho, t_{\rho+1}]$, it derives

$$\dot{V}(t) \leq -y_{zi}(t)^Ty_{zi}(t) + \gamma^2\omega_i(t)^T\omega_i(t)$$

Since $\dot{V}(t)$ is continuous in t, the integration of both sides from 0 to $+\infty$ yields

$$V(+\infty) - V(0) \leq \int_0^{+\infty}[-y_{zi}(t)^Ty_{zi}(t) + \gamma^2\omega_i(t)^T\omega_i(t)]dt.$$

Under the zero initial condition $V(0) = 0$, one can derive

$$\int_0^{+\infty} y_{zi}(t)^Ty_{zi}(t)dt \leq \int_0^{+\infty} \gamma^2\omega_i(t)^T\omega_i(t)dt.$$

that is, $\|y_{zi}(t)\| \leq \gamma\|\omega_i(t)\|$ for any nonzero $\omega_i(t) \in \mathcal{L}_2[0, +\infty]$. Then, with a condition that $\omega_i(t) = 0$, system (15) is asymptotically stable based on the proof in Theorem 1, from which we can confirm that system (15) is asymptotically stable with an H_∞ performance index γ. This

completes the proof.

Proof of incorrect theorem in [16]

The Lyapunov functional constructed in [16] are shown as follows:

$$\begin{aligned}V(t) &= x^T(t)Px(t) + \int_{t-\tau_M}^{t} x(s)Qx(s)ds \\ &+ \int_{t-\tau_M}^{t}\int_{\eta}^{t} \dot{x}^T(s)R\dot{x}(s)dsd\eta \\ &+ (\bar{\tau}-\tau(t))[x(t)-x(t-\tau(t))]^T\mathbb{W}[x(t)-x(t-\tau(t))] \\ &+ (\bar{\tau}-\tau(t))\int_{s_k}^{t}\dot{x}^T(s)\mathbb{Z}\dot{x}(s)ds\end{aligned}$$

where, the corresponding notations are defined in [16]. Then, we can find that the classical functional part is

$$\begin{aligned}V_1(t) &= x^T(t)Px(t) + \int_{t-\tau_M}^{t} x(s)Qx(s)ds \\ &+ \int_{t-\tau_M}^{t}\int_{\eta}^{t} \dot{x}^T(s)R\dot{x}(s)dsd\eta\end{aligned}$$

The looped Lyapunov functional part is

$$\begin{aligned}V_2(t) &= (\bar{\tau}-\tau(t))[x(t)-x(t-\tau(t))]^T\mathbb{W}[x(t)-x(t-\tau(t))] \\ &+ (\bar{\tau}-\tau(t))\int_{s_k}^{t}\dot{x}^T(s)\mathbb{Z}\dot{x}(s)ds\end{aligned}$$

Note that the classical part is continuous on $t \in [0, +\infty)$, while the looped part is continuous on $t \in [0, +\infty)$ except for the discontinuous instants $s_k = t_k + \tau_k, k = 0, 1, 2\cdots$. Based on the derivation in [44], to prove the stability of the system, the selected looped Lyapunov functional $V_2(t)$ needs to meet the following condition at the discontinuous instants (or jump points):

$$\lim_{t\to s_k^-} V_2(t) \geq V_2\left(s_k^+\right) \tag{27}$$

Or the following improved conditions in [33],

$$V_2(s_k) = V_2(s_{k+1}). \tag{28}$$

According to the careful derivation, one can obtain

$$\begin{aligned}\lim_{t\to s_k^-} V_2(t) &= (\bar{\tau}-(t_k-t_{k-1}+\tau_k))\left[x\left(s_k^-\right)-x\left(t_{k-1}\right)\right]^T\mathbb{W} \\ &\times\left[x\left(s_k^-\right)-x\left(t_{k-1}\right)\right]\geq 0\end{aligned}$$

$$V_2\left(s_k^+\right) = (\bar{\tau}-\tau_k)\left[x\left(s_k^+\right)-x\left(t_k\right)\right]^T\mathbb{W}\left[x\left(s_k^+\right)-x\left(t_k\right)\right]\geq 0$$

Since the relationship between $x(t_k)$ and $x(t_{k-1})$ cannot be determined, $\lim_{t\to s_k^-} V_2(t)$ and $V_2\left(s_k^+\right)$ may not meet the condition (27). On the other hand, through a similar derivation, one can obtain

$$V_2\left(s_k\right) = (\bar{\tau}-\tau_k)\left\{\left[x\left(s_k\right)-x\left(t_k\right)\right]^T\mathbb{W}\left[x\left(s_k\right)-x\left(t_k\right)\right]\right\}\geq 0$$

$$\begin{aligned}V_2\left(s_{k+1}\right) &= \left(\bar{\tau}-\left(t_{k+1}-t_k+\tau_{k+1}\right)\right)\left[x\left(s_{k+1}\right)-x\left(t_k\right)\right]^T\mathbb{W} \\ &\times\left[x\left(s_{k+1}\right)-x\left(t_k\right)\right]\geq 0\end{aligned}$$

Since the relationship between $x(s_k)$ and $x(s_{k+1})$ cannot be determined, $V_2\left(s_k\right)$ and $V_2\left(s_{k+1}\right)$ may not meet the condition (28). Therefore, the Lyapunov functional constructed in [16] is not correct and results in incorrect stability condition.

References

[1] A. Latif, S.M. S. Hussain and D. C. Das, "State-of-the-art of controllers and soft computing techniques for regulated load frequency management of single/multi-area traditional and renewable energy based power systems," *Appl. Energ.*, vol. 266, pp. 114858, May 2020.

[2] C. Chen, M. Cui, X. Fang, B. Ren and Y. Chen, "Load altering attack-tolerant defense strategy for load frequency control system," *Appl. Energ.*, vol. 280, pp. 116015, Dec. 2020.

[3] C. K. Zhang, L. Jiang, Q. H. Wu, Y. He and M. Wu, "Delay-dependent robust load frequency control for time delay power systems," *IEEE Trans. Power Syst.*, vol. 28, no. 3, pp. 2192–2201, Aug. 2013.

[4] S. K. Pandey, S. R. Mohanty and N. Kishor. "A literature survey on load¨Cfrequency control for conventional and distribution generation power systems," *Renew. Sust. Energ. Rev.*, vol. 25, pp. 318–334, Sept. 2013.

[5] K. Tomsovic, D. E. Bakken, V. Venkatasubramanian and A. Bose, "Designing the next generation of real-time control, communication, and computations for large power systems," *Proceedings of the IEEE*, vol. 93, no. 5, pp. 965–979, May 2005.

[6] S. Bhowmik, K. Tomsovic and A. Bose, "Communication models for third party load frequency control," *IEEE Trans. Power Syst.*, vol. 19, no. 1, pp. 543-548, Feb. 2004.

[7] C. Peng, J. Li and M. Fei, "Resilient event-triggering H_∞ load frequency control for multi-area power systems with energy-limited dos attacks," *IEEE Trans. Power Syst.*, vol. 32, no. 5, pp. 4110–4118, Sept. 2017.

[8] L. Dong, Y. Tang, H. He and C. Sun, "An event-triggered approach for load frequency control with supplementary ADP," *IEEE Trans. Power Syst.*, vol. 32, no. 1, pp. 581–589, Jan. 2017.

[9] V. C. Gungo, D. Sahin, T. Kocak, S. Ergut, C. Buccella, C. Cecati, et al., "Smart grid technologies: Communication technologies and standards," *IEEE Trans. Ind. Inf.*, vol. 7, no. 4, pp. 529–539, Nov. 2011.

[10] C. Li, X. Yu, W. Yu, T. Huang and Z.-W. Liu, "Distributed event-triggered scheme for economic dispatch in smart grids," *IEEE Trans. Ind. Inf.*, vol. 12, no. 5, pp. 1775–1785, Oct. 2016

[11] Y. Wang, I. R. Pordanjani and W. Xu, "An event-driven demand response scheme for power system security enhancement," *IEEE Trans. Smart Grid*, vol. 2, no. 1, pp. 23–29, March 2011.

[12] X. C. Shangguan, Y. He, C. K. Zhang, L. Jin, W. Yao, L. Jiang and M. Wu,, " Control performance standards-oriented event-triggered load frequency control for power systems under limited communication bandwidth," *IEEE Trans. Control Syst. Technol.*, 2021, to be pubished. Doi:10.1109/TCST.2021.3070861.

[13] C. Yang, W. Yao, J. Fang, X. Ai, Z. Chen, J. wen, et al., "Dynamic event-triggered robust secondary frequency control for islanded AC microgrid," *Appl. Energ.*, vol. 242, pp. 821–836, May 2019.

[14] A. H. Hosseinloo, A. Ryzhov, A. Bischi, H. Ouerdane, K. Turitsyn and M. A. Dahlehet, "Data-driven control of micro-climate in buildings: An event-triggered reinforcement learning approach," *Appl. Energ.*, vol. 277, pp. 115451, Nov. 2020.

[15] X. Liu, L. Li, Z. Li, X. Chen, T. Fernando, H. H.-C. Iu, et al., "Event-trigger particle filter for smart grids with limited communication bandwidth infrastructure," *IEEE Trans. Smart Grid*, 2017, vol. 9, no. 6, pp. 6918–6928, Nov. 2018.

[16] S. Wen, X. Yu, Z. Zeng and J. Wang, "Event-triggering load frequency control for multi-area power systems with communication delays," *IEEE Trans. Ind. Electron.*, vol. 63, no. 2, pp. 1308–1317, Feb. 2016.

[17] S. Saxena and E. Fridman, "Event-Triggered load frequency control via switching approach," *IEEE Trans. Power Syst.*, vol. 35, no. 6, pp. 4484–4494, Nov. 2020.

[18] Q. Wang, and Y. He, "Time-triggered intermittent control of continuous systems," *Int. J. Robust Nonlinear Control*, vol. 31, no. 14, pp. 6867–6879, Sept. 2021.

[19] L. Jin, Y. He, C. K. Zhang, X. C. Shangguan, L. Jiang and M. Wu, "Novel structure-exploiting techniques based delay-dependent stability analysis of multi-area LFC with improved numerical tractability," *IEEE Trans. Power Syst.*, vol. 36, no. 5, pp. 4194–4211, Sept. 2021.

[20] H. Luo, I. A. Hiskens and Z. Hu, "Stability analysis of load frequency control systems with sampling and transmission delay," *IEEE Trans. Power Syst.*, vol. 35, no. 5, pp. 3603–3615, Sept. 2020.

[21] C. Peng and J. Zhang, "Delay-distribution-dependent load frequency control of power systems with probabilistic interval delays," *IEEE Trans. Power Syst.*, vol. 31, no. 4, pp. 3309–3317, July 2016.

[22] P. B. Andersen, S. H. Toghroljerdi, T. M. Sorensen, B. E. Christensen, J. C. M. L. Hoj and A. Zecchino, "The parker project," *Final Report*, Jan. 2019.

[23] L. Jiang, W. Yao, Q. H. Wu, J. Y. Wen and S. J. Cheng, "Delay-dependent stability for load frequency control with constant and time-varying delays," *IEEE Trans. Power Syst.*, vol. 27, no. 2, pp. 932–941, May 2012.

[24] F. Yang, J. He and Q. Pan, "Further improvement on delay-dependent load frequency control of power systems via truncated B¨CL inequality," *IEEE Trans. Power Syst.*, vol. 33, no. 5, pp. 5062–5071, Sept. 2018.

[25] J. Nanda, A. Mangla and S. Suri, "Some new findings on automatic generation control of an interconnected hydrothermal system with conventional controllers," *IEEE Trans. Energy Convers.*, vol. 21, no. 1, pp. 187–194, March 2006.

[26] C. Peng, J.Zhang and H. Yan, "Adaptive event-triggering H_∞ load frequency control for network-based power systems," *IEEE Trans. Ind. Electron.*, vol. 65, no. 2, pp. 1685–1694, Feb. 2018.

[27] H. Zhang, S. Su, Y. Y. Zhao and J. Lu, "Networked load frequency control of multi-area uncertain power systems via adaptive event-triggered communication scheme," *J. Franklin Inst.*, vol. 356, no. 16, pp. 9600–9626. Nov. 2019.

[28] X. Su, X. Liu and Y. D. Song, "Event-triggered sliding-mode control for multi-area power systems," *IEEE Trans. Ind. Electron.*, vol. 64, no. 8, pp. 6732–6741, Aug. 2017.

[29] V. P. Singh, N. Kishor and P. Samuel, "Distributed multi-agent system-based load frequency control for multi-area power system in smart grid," *IEEE Trans. Ind. Electron.*, vol. 64, no. 6, pp. 5151–5160, June 2017.

[30] S. Liu, W. Luo and L. Wu, "Co-design of distributed model-based control and event-triggering scheme for load frequency regulation in smart grids," *IEEE Trans. Syst. Man Cybern. Syst.*, vol. 50, no. 9, pp. 3311–3319, Sept. 2020.

[31] Y. Liu, Y. Chen and M. Li, "Dynamic event-based model predictive load frequency control for power systems under cyber attacks," *IEEE Trans. Smart Grid*, 2020, to be pubished. Doi: 10.1109/TSG.2020.3022094.

[32] J. Liu, Y. Gu, Y. Liu and J. Cao, "Event-triggered H_∞ load frequency control for multiarea power systems under hybrid cyber attacks," *IEEE Trans. Syst. Man Cybern. Syst.*, vol. 49, no. 8, pp. 1665–1678, Aug. 2019.

[33] A. Seuret, " A novel stability analysis of linear systems under asynchronous samplings," *Automatica*, vol. 48, no. 1, pp. 177–182, Jan. 2012.

[34] K. Liu and E. Fridman, "Wirtinger's inequality and Lyapunov-based sampled-data stabilization," *Automatica*, vol. 48, no. 1, pp. 102–108, Jan. 2012.

[35] H. B. Zeng, K. L. Teo and Y. He, "A new looped-functional for stability analysis of sampled-data systems," *Automatica*, vol. 82, pp. 328–331, Aug. 2017.

[36] X. C. Shangguan, Y. He, C. K. Zhang, L. Jiang, J. W. Spencer and M. Wu, "Sampled-data based discrete and fast load frequency control for power systems with wind power," *Appl. Energ.*, vol. 259, pp. 114202, Feb. 2020.

[37] X. C. Shangguan, C. K. Zhang, Y. He, L. Jin, L. Jiang, J. W. Spencer, et al., "Robust load frequency control for power system considering transmission delay and sampling period," *IEEE Trans. Ind. Inf.*, vol. 17, no. 8, pp. 5292–5303, Aug. 2021

[38] F. Yang, J. He and D.Wang, "New stability criteria of delayed load frequency control systems via infinite-series-based inequality," *IEEE Trans. Ind. Inf.*, vol. 14, no. 1, pp. 231–240, Jan. 2018.

[39] K. Ramakrishnan and G. Ray,"Stability criteria for nonlinearly perturbed load frequency systems with time-delay," *IEEE J. Emerging Sel. Top. Circuits Syst.*, vol. 5, no. 3, pp. 383–392, Sept. 2015.

[40] A. Seuret and F. Gouaisbaut, "Wirtinger-based integral inequality: Application to time-delay systems," *Automatica*, vol. 49, no. 9, pp. 2860–2866, Sept. 2013.

[41] I. Hiskens, "IEEE PES task force on benchmark systems for stability controls", *Tech. Rep. 39-bus system*, 2013.

[42] C. Hua, S. Wu and X. Guan, "Stabilization of TS fuzzy system with time delay under sampled-data control using a new looped-functional," *IEEE Trans. Fuzzy Syst.*, vol. 28, no. 2, pp. 400–407, Feb. 2020.

[43] J. Chen, J. H. Park and S. Xu, "Stability analysis for delayed neural networks with an improved general free-matrix-based integral inequality," *IEEE Trans. Neural Netw. Learn. Syst.*, vol. 31, no. 2, pp. 675–684, Feb. 2020.

[44] C. Hua, C. Ge and X. Guan, "Synchronization of chaotic Lur'e systems with time delays using sampled-data control," *IEEE Trans. Neural Netw. Learn. Syst.*, vol. 26, no. 6, pp. 1214–1221, June 2015.